

Modeling the Impacts of Wintertime Arctic Leads Upon the Atmosphere

Michael A. Zulauf and Steven K. Krueger

Department of Meteorology
University of Utah
Salt Lake City, UT 84112

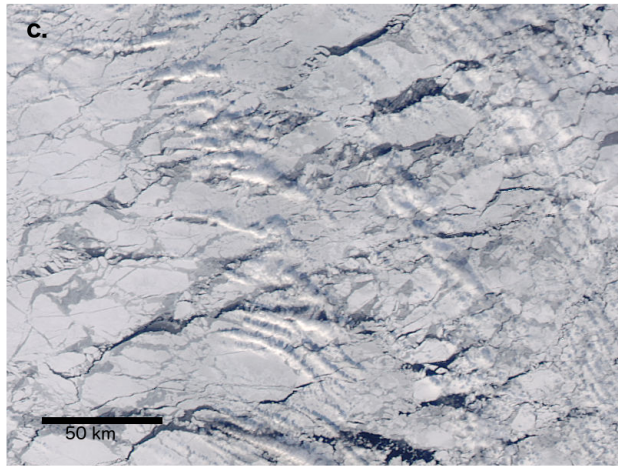


Figure 1: (a) Aerial photo of sea ice leads near Barrow, Alaska. Photo by Lars Kaleschke, published on phys.org. (b) Aerial photo of lead-generated clouds. Photo by T. Arbetter, University of Colorado. (c) MODIS image from northern Sea of Okhotsk on 8 February 2016, published on nasa.gov. Lead-modulated clouds are prominently visible over the left half of this image.

Arctic Leads

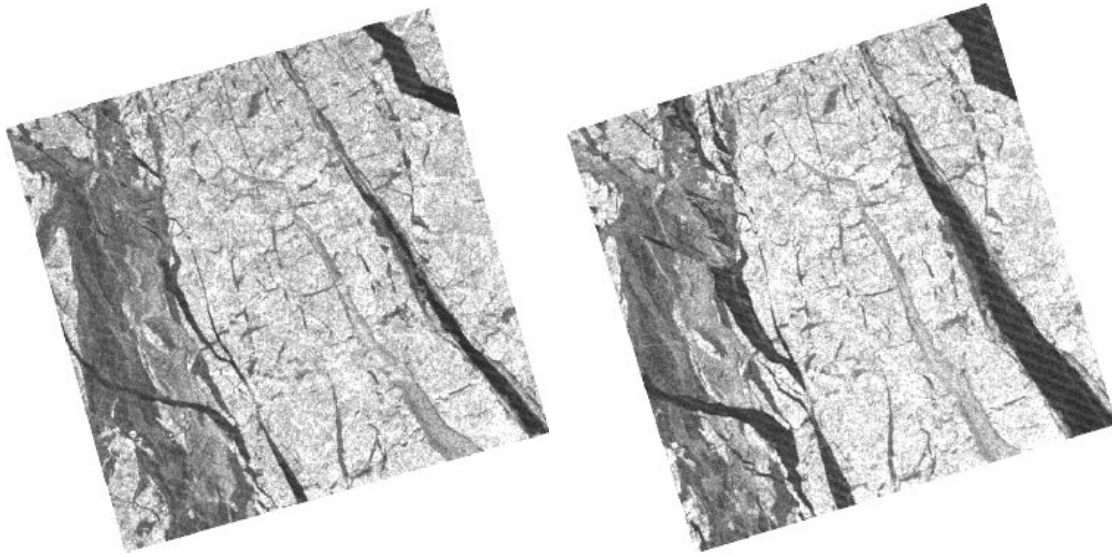


Lead and associated plume. Photo taken on BASE flight 16, October 12, 1994, over the Beaufort Sea.

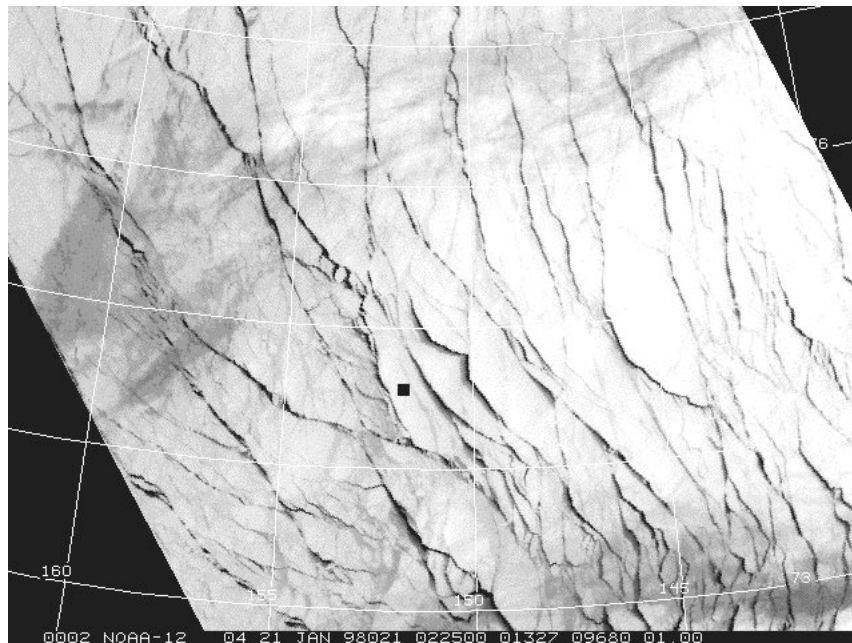
Motivation:

- Extreme temperature differences between open water and winter atmosphere may result in surface fluxes up two orders of magnitude greater than those from snow/ice surface
- Thus, leads may have a significant impact upon the Arctic climate.
- Small-scale features such as leads can't be directly resolved by large-scale models

Remote Sensing of Leads at SHEBA



60 km x 60 km SAR images from January 17 and January 20, 1998 (rotated so north is at top). Copyright ©1998 by Canadian Space Agency.



NOAA-14 1 km high resolution IR image from January 21, 1998. Image provided to SHEBA by SSEC at the University of Wisconsin.

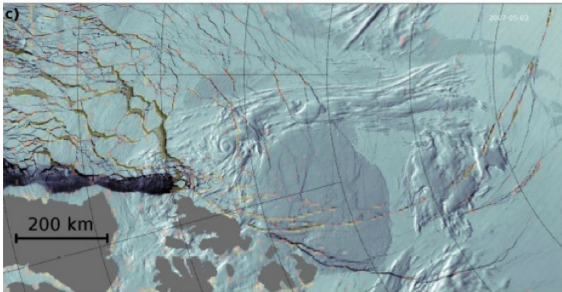


Figure 3: Gray-scale thin ice concentrations (TIC, i.e., leads) derived from AMSR-E overlaying the MODIS band 3 of 1 km pixel size, with leads visible as dark linear objects. One can easily see that TIC matches MODIS well for wider leads but not narrower ones.

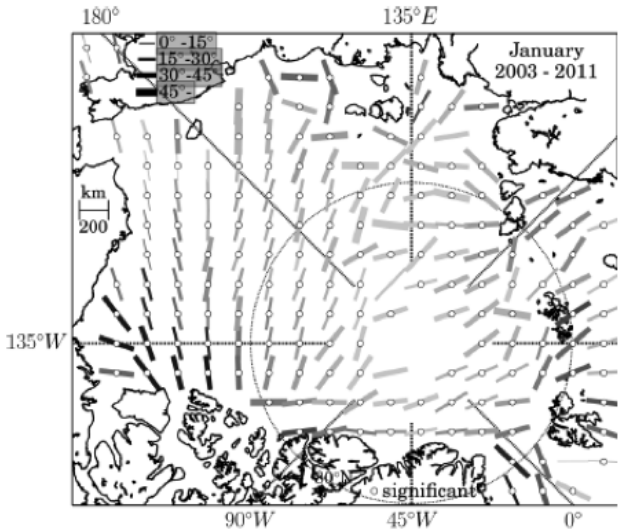


Figure 4: January mean lead orientation for 2003-2011. On each symbol, grey shading indicates the number of leads and bar width indicates the standard deviation of all lead orientations in a $200 \text{ km} \times 200 \text{ km}$ cell. White dots on top of a line indicate that the lead orientations are distributed on a confidence level of 99%. Adapted from (Brohan and Kaleschke 2014).

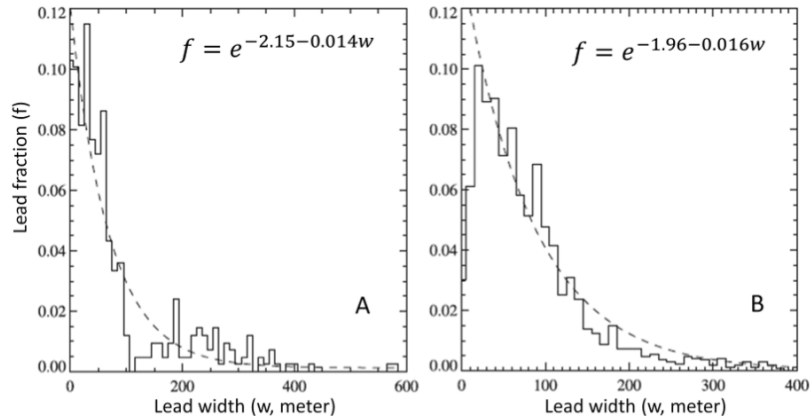


Figure 2: Lead width distribution (exponential function) in the SHEBA region for 24 May 1998, derived from **a** Airborne Imaging Microwave Radiometer (AIMR) (using the 90 GHz channel) and high spatial resolution video observations, and derived from **b** AVHRR. Adapted from (*Tschudi et al. 2002*)

Physics:

A number of factors may influence plume development, and thus the enhanced surface fluxes

- **ambient wind speed and orientation** (magnitude of fluxes, Brunt Väisälä period)
- **lead width** (total heat released, Brunt Väisälä period, enhanced surface wind feedback)
- **latent heating & liquid/ice microphysics** (release of additional heat to the plume)
- **cloud cover and radiative forcing** (winter—IR only)
- **atmospheric temperature and stability**
- **lead refreezing** (air-lead temperature difference)

Plume penetration height

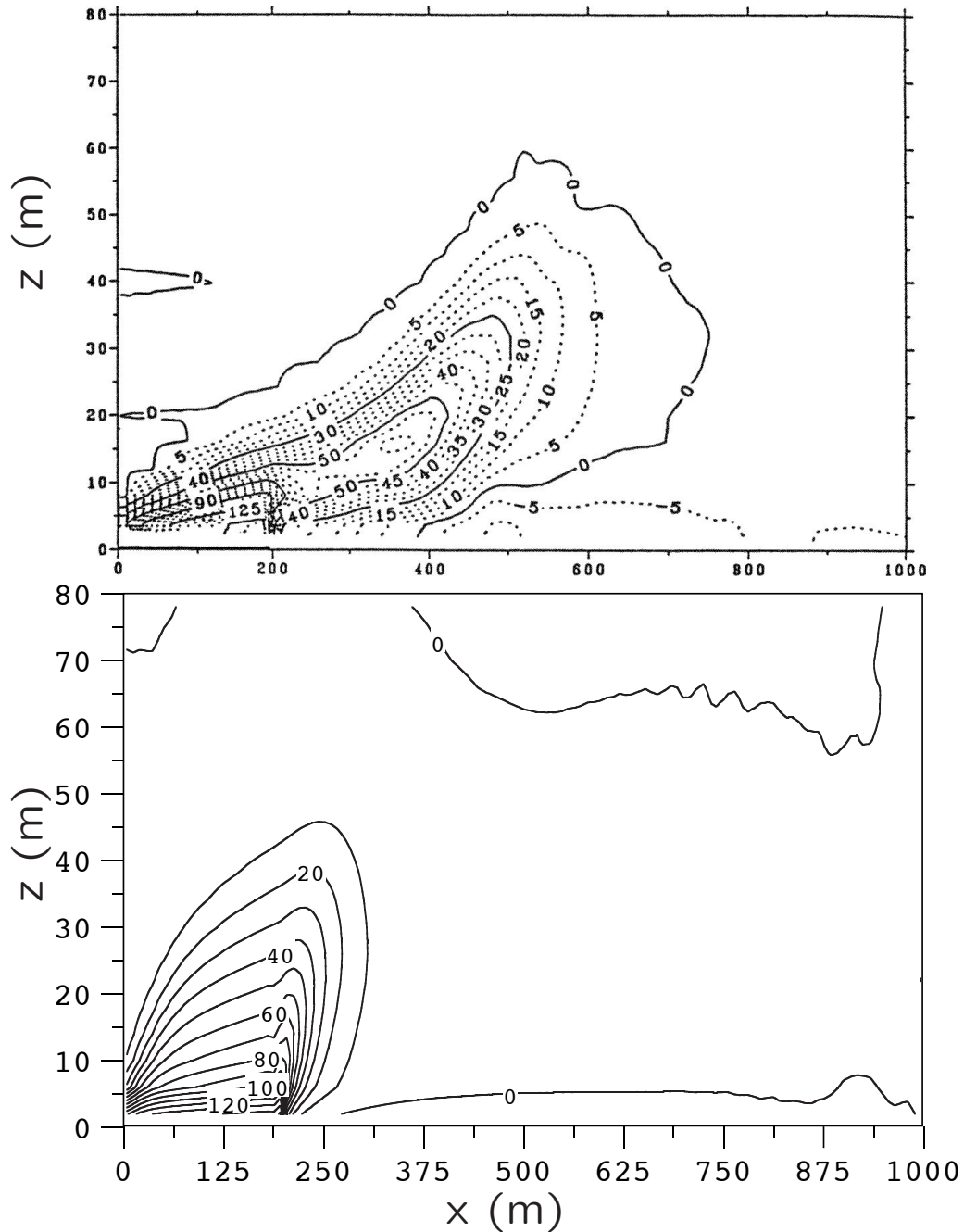
- Plume height determines the depth of the layer affected by the lead's convective fluxes.
- Prediction requires a plume model.
- Primary input is the integrated surface buoyancy flux, which can strongly depend on the plume circulation itself.
- Prediction is not possible using a 1D boundary layer model.

University of Utah Cloud-Resolving Model

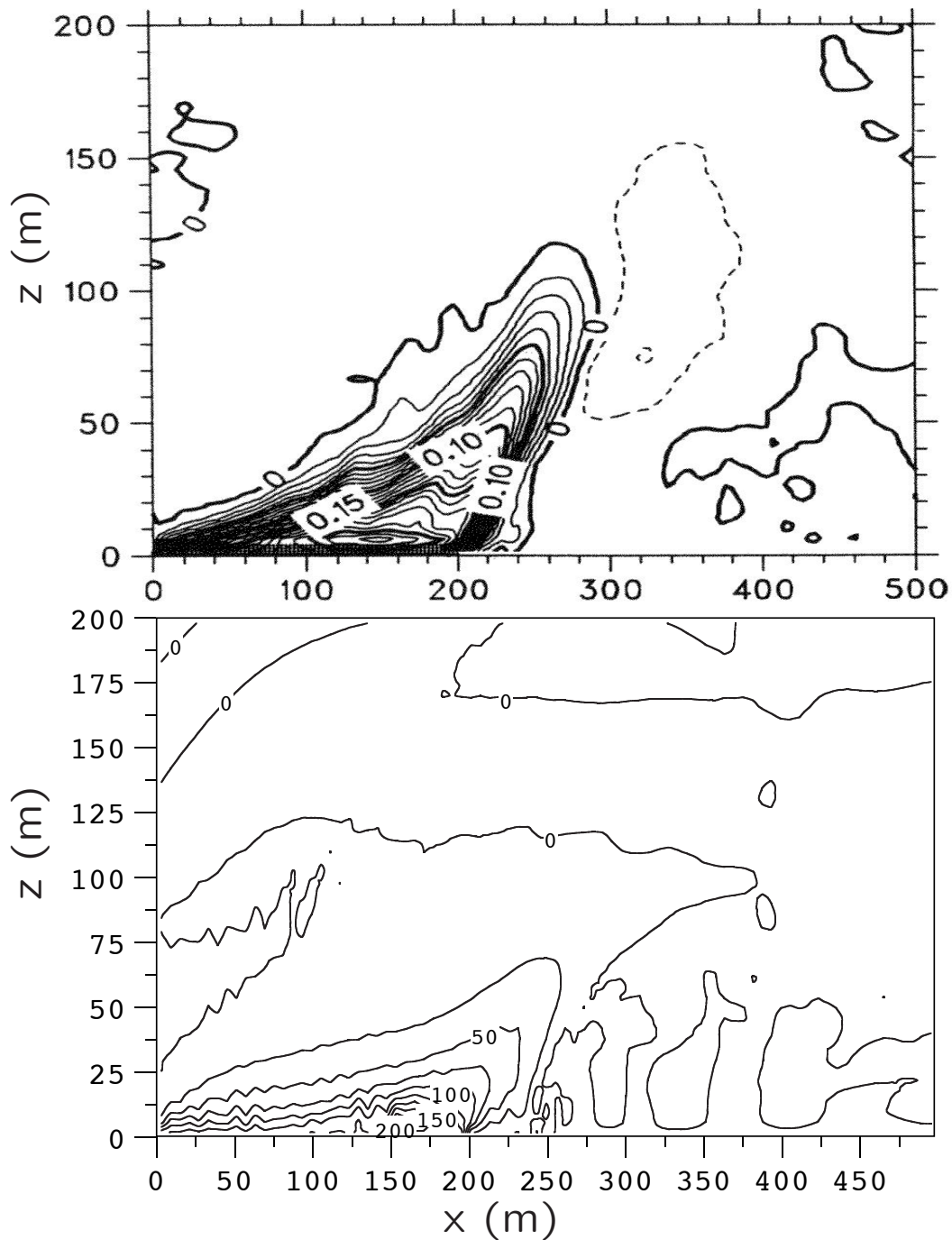
- 2-D non-hydrostatic resolved dynamics
- third-moment turbulence closure
- Fu-Liou radiative transfer code
- stability-dependent surface fluxes
- three phase bulk cloud microphysics

Basic Simulation Parameters (as in Glendening and Burk, 1992)

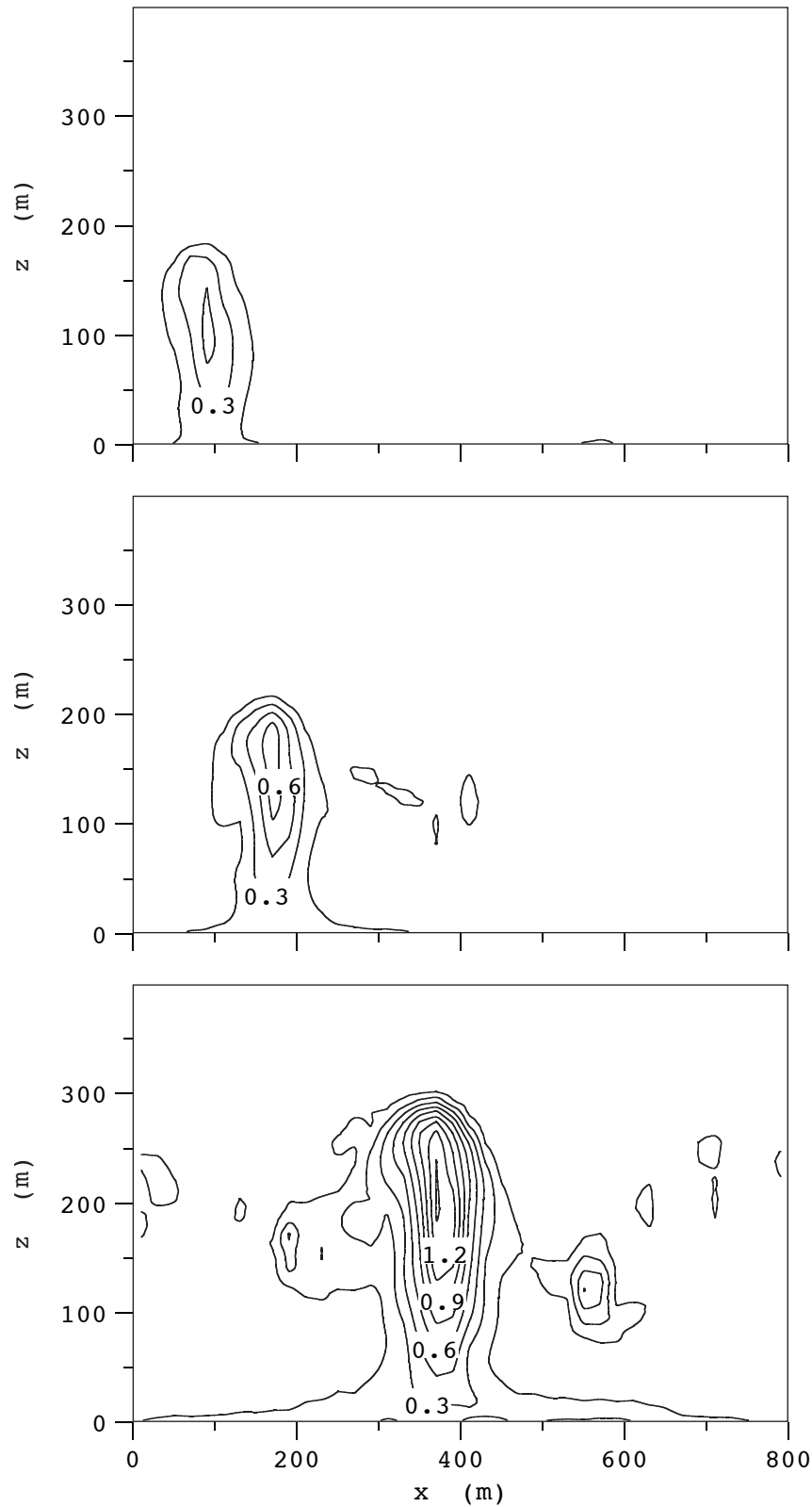
- $\partial\theta/\partial z = 10 \text{ K km}^{-1}$
- surface air temperature of -27°C
- ice temperature of -29°C
- water temperature of -2°C
- geostrophic wind of 2.5 m s^{-1} (varying orientation)
- latitude of 79°N



Mean total vertical turbulent temperature flux (K m s^{-1} , scaled by 10^3) for a 200 m lead, **90° wind orientation**: GB92 (top), CRM (bottom).

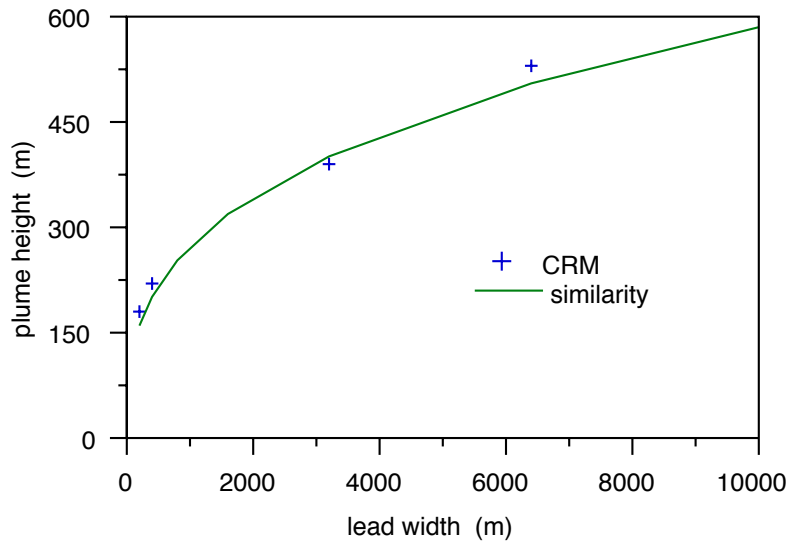


Mean total vertical turbulent temperature flux (K m s^{-1}) for a 200 m lead, **15° wind orientation**: G94 (top), CRM (bottom, scaled by 10^3).

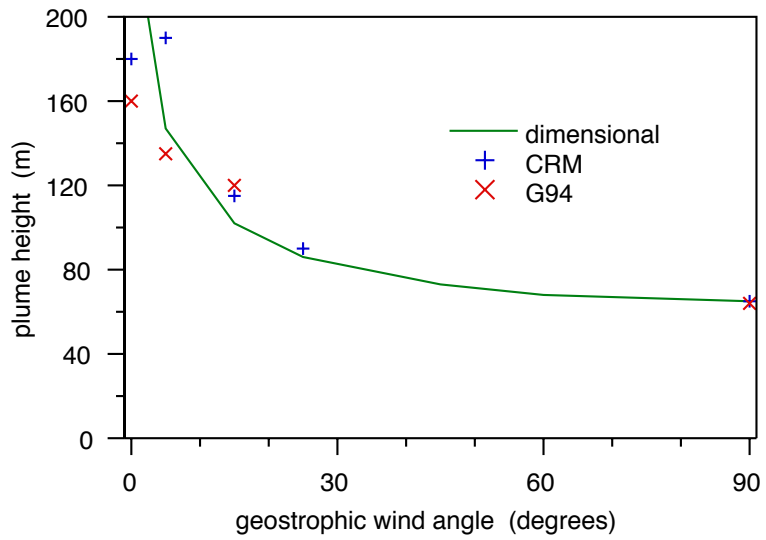


Mean total turbulent kinetic energy ($\text{m}^2 \text{s}^{-2}$) for a 200 m (top), 400 m (middle), and 800 m (bottom) lead.

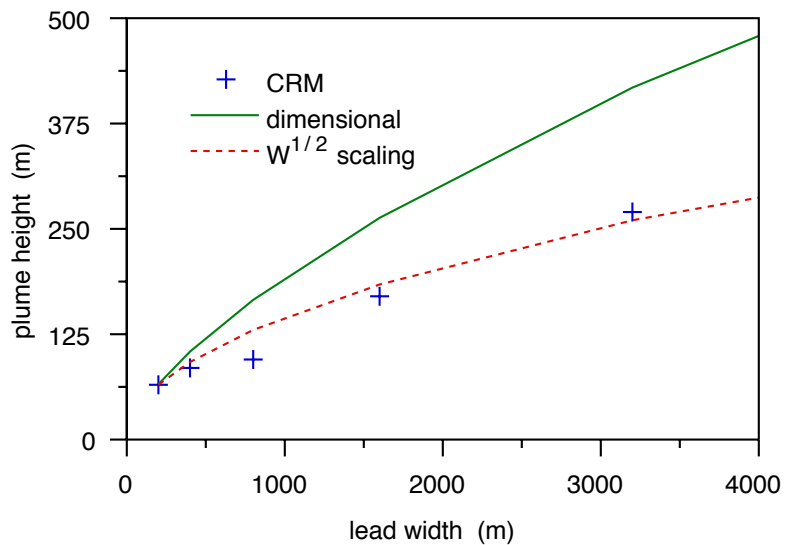
- no cross wind, varying width



- constant width, varying wind angle



- cross wind, varying width



Analytical Expressions for Plume Penetration Height

- For cases where there is **no large-scale cross-lead wind**, a similarity solution can be obtained as in Emanuel (1994).

With constant, stable stratification, it simplifies to:

$$h \sim F_0^{1/3} N^{-1}$$

where: $F_0 \equiv$ buoyancy flux at surface

$$N^2 \equiv g/\theta_0 \partial\theta/\partial z \quad (N = \text{Brunt Väisälä frequency})$$

- For cases where there is **significant large-scale cross-lead wind**, Glendening and Burk (1992), using dimensional arguments, derived a modified expression:

$$h \sim F_0^{1/3} N^{-1} \left(\frac{W}{U} N \right)^{1/3}$$

where: $W \equiv$ lead width

$U \equiv$ cross-lead wind component

For case with no cross-lead wind: $h \sim W^{1/3}$

For case with cross-lead wind: $h \sim W^{2/3}$

Given a lead's width, orientation, and ice thickness (of freezing leads), we can estimate the integrated surface buoyancy flux, F , over the lead from large-scale atmospheric conditions using the fetch-dependent flux formulation described in *Andreas and Cash* (1999). Therefore, if the joint distributions of lead width, orientation, and ice thickness are known, or can be parameterized, we can estimate the plume height distribution, as well as the ensemble plume mass flux and mass detrainment rate profiles. The mass flux profile (per unit lead length) for a plume from a lead with integrated buoyancy flux F_i in an unstratified atmosphere is

$$M_i(F_i, z) = 1.8 (\pi/32)^{1/2} \rho(z) F_i^{1/3} z, \quad (3)$$

where ρ is the air density (*Emanuel* 1994). This formula is approximately valid even in a stratified atmosphere at levels below the non-buoyancy level where entrainment is the dominant buoyancy-decreasing process. We will apply (3) up to the non-buoyancy level, where the mass flux vanishes. The detrainment rate, D_i , is simply M_i at the non-buoyancy level. Note that both M_i and D_i depend on lead width through the integrated buoyancy flux F_i .

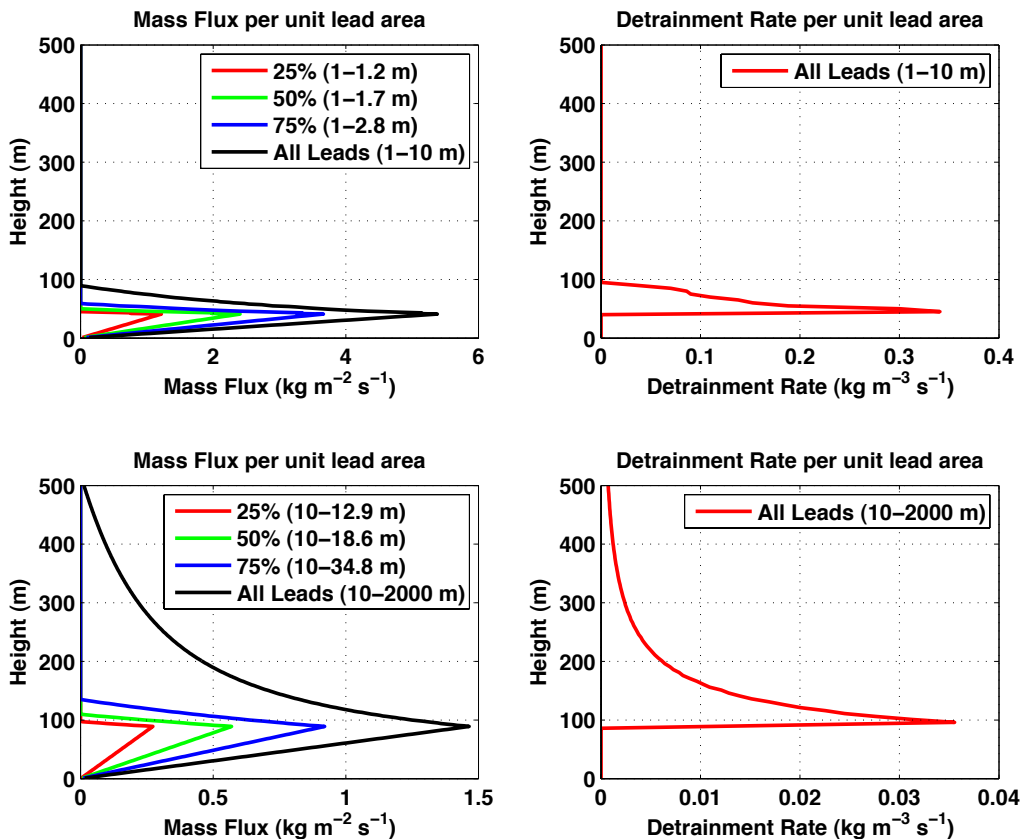


Figure 8: Ensemble plume mass flux and mass detrainment rate profiles, for an ensemble of leads with a width distribution described by (8) with $a = 2.1$, plume height calculated by (1), and with $F = 1000 \text{ W m}^{-2}$ and $N = 0.02 \text{ s}^{-1}$.

The large-scale effects of the penetrating convective plumes include heating and drying due to plume-induced subsidence as well as moistening and cloud generation due to detrainment (*Arakawa and Schubert 1974*). The large-scale tendencies of potential temperature, θ , water vapor mixing ratio, q_v , and cloud ice mixing ratio, q_i , due to an ensemble of penetrating convective plumes are

$$\rho \frac{\partial \bar{\theta}}{\partial t} = M \frac{\partial \bar{\theta}}{\partial z} + D(\hat{\theta} - \bar{\theta}), \quad (4)$$

$$\rho \frac{\partial \bar{q}_v}{\partial t} = M \frac{\partial \bar{q}_v}{\partial z} + D(\hat{q}_v - \bar{q}_v), \quad (5)$$

$$\rho \frac{\partial \bar{q}_i}{\partial t} = M \frac{\partial \bar{q}_i}{\partial z} + D(\hat{q}_i - \bar{q}_i), \quad (6)$$

where M is the ensemble plume mass flux and D is the ensemble plume detrainment rate. Both are calculated from (3) and the frequency distribution of lead widths.

- There exist a number of feedbacks which can alter the magnitude of the surface fluxes over the lead, and thus the plume penetration height:
 1. lead width \Rightarrow circulation strength (+)
 2. lead width \Rightarrow vertical mixing (+)
 3. lead width \Rightarrow near-surface air temperature (-)

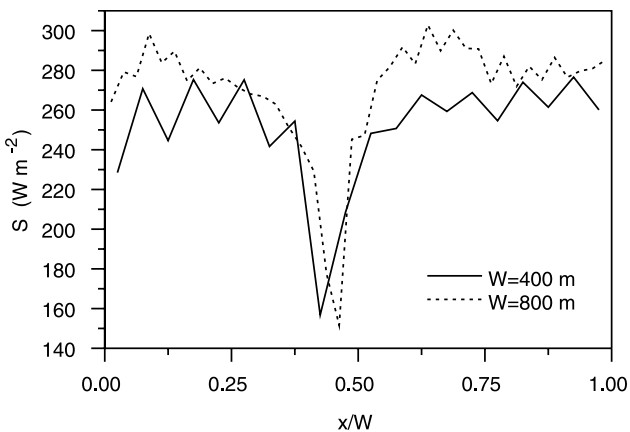
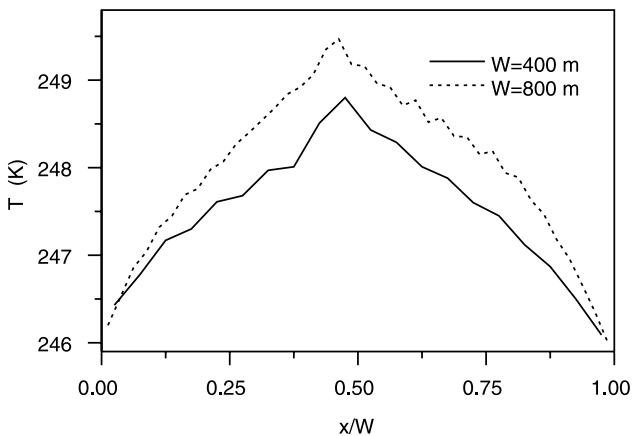
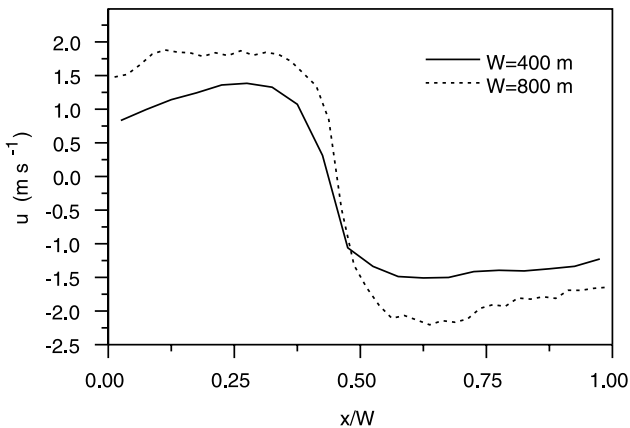


Figure 7. Comparison of near-surface inflow wind speed (top), near-surface air temperature (middle), and surface sensible heat fluxes (bottom) as a function of fractional lead width for 400 and 800 m leads with lead parallel large-scale wind.

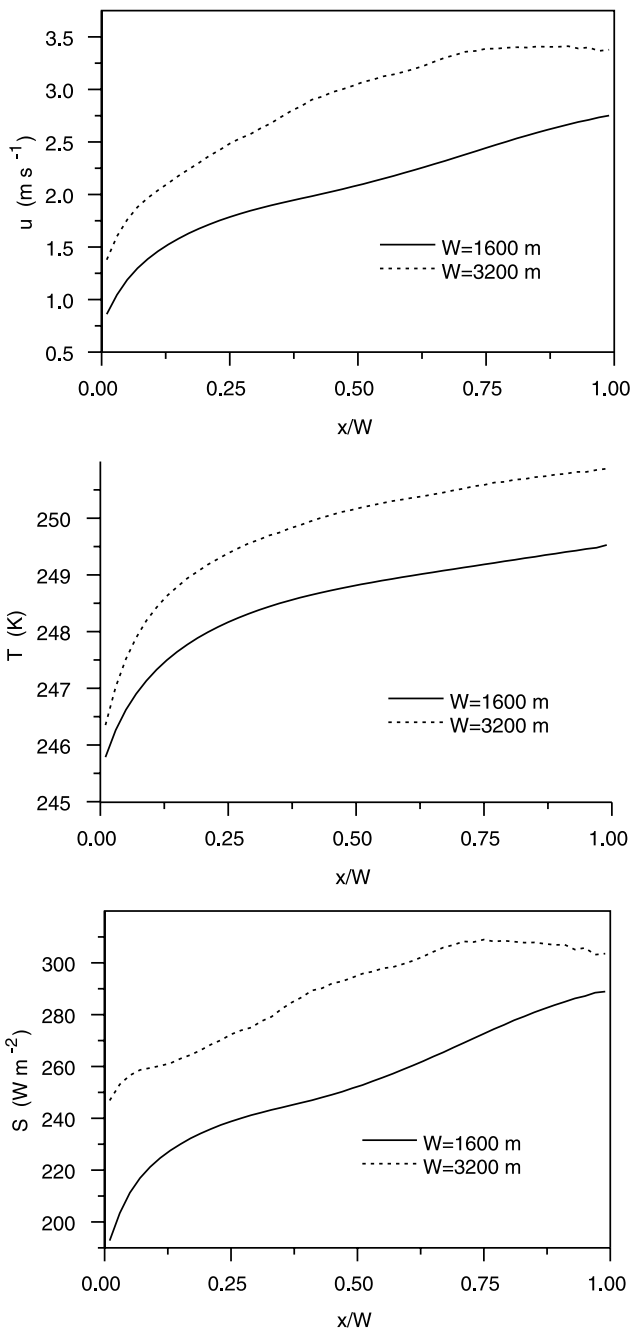


Figure 9. Comparison of near-surface inflow wind speed (top), near-surface air temperature (middle), and surface sensible heat fluxes (bottom) as a function of fractional lead width for 1600 and 3200 m leads with large-scale cross-lead wind.

Table 1. Impact of Lead Width (W) on Plume Height (h) and Surface Sensible Heat Flux (S) for Cases With Large-Scale Cross-Lead Wind

W , m	h , m	S , $W\ m^{-2}$
100	~ 55	241
200	~ 65	244
400	~ 85	248
800	~ 95	253
1600	~ 170	253
3200	~ 270	289

- The inclusion of microphysical and radiative processes can increase plume penetration height minimally for narrow leads, more so for wider leads.

Table 2. Impact of Additional Physics Upon Plume Penetration Height for Various Lead Widths^a

W , m	h_{dry} , m	h_{moist} , m	h_{rad} , m
200	~180	~185	~190
400	~220	~235	~240
3200	~430	~460	~475
6400	~580	~650	~710

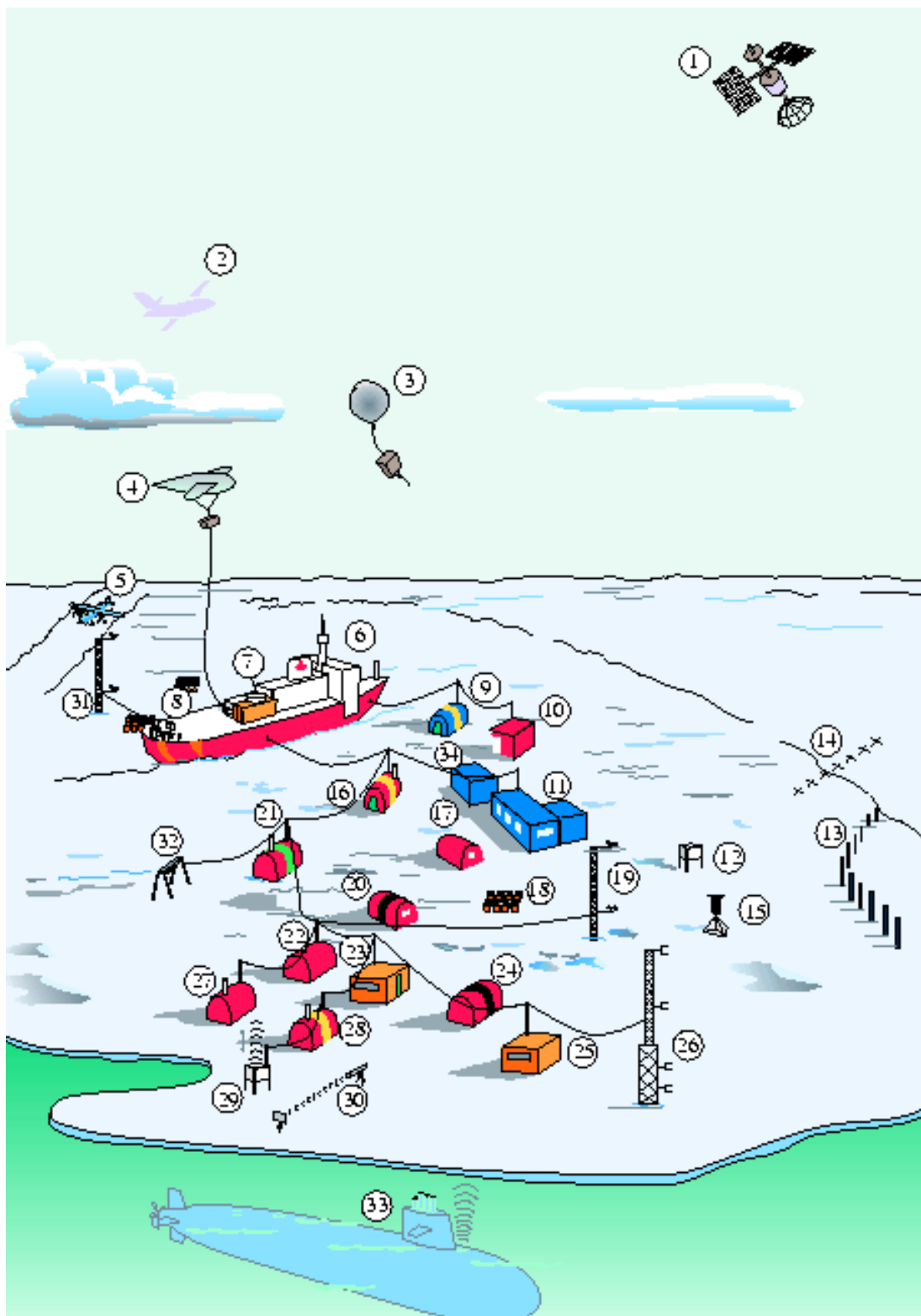
^aFor cases with no large-scale cross-lead wind.

Table 3. Results From CRM Simulations and Parameterizations for the Basic “Dry,” “Moist,” and “Rad” Cases^a

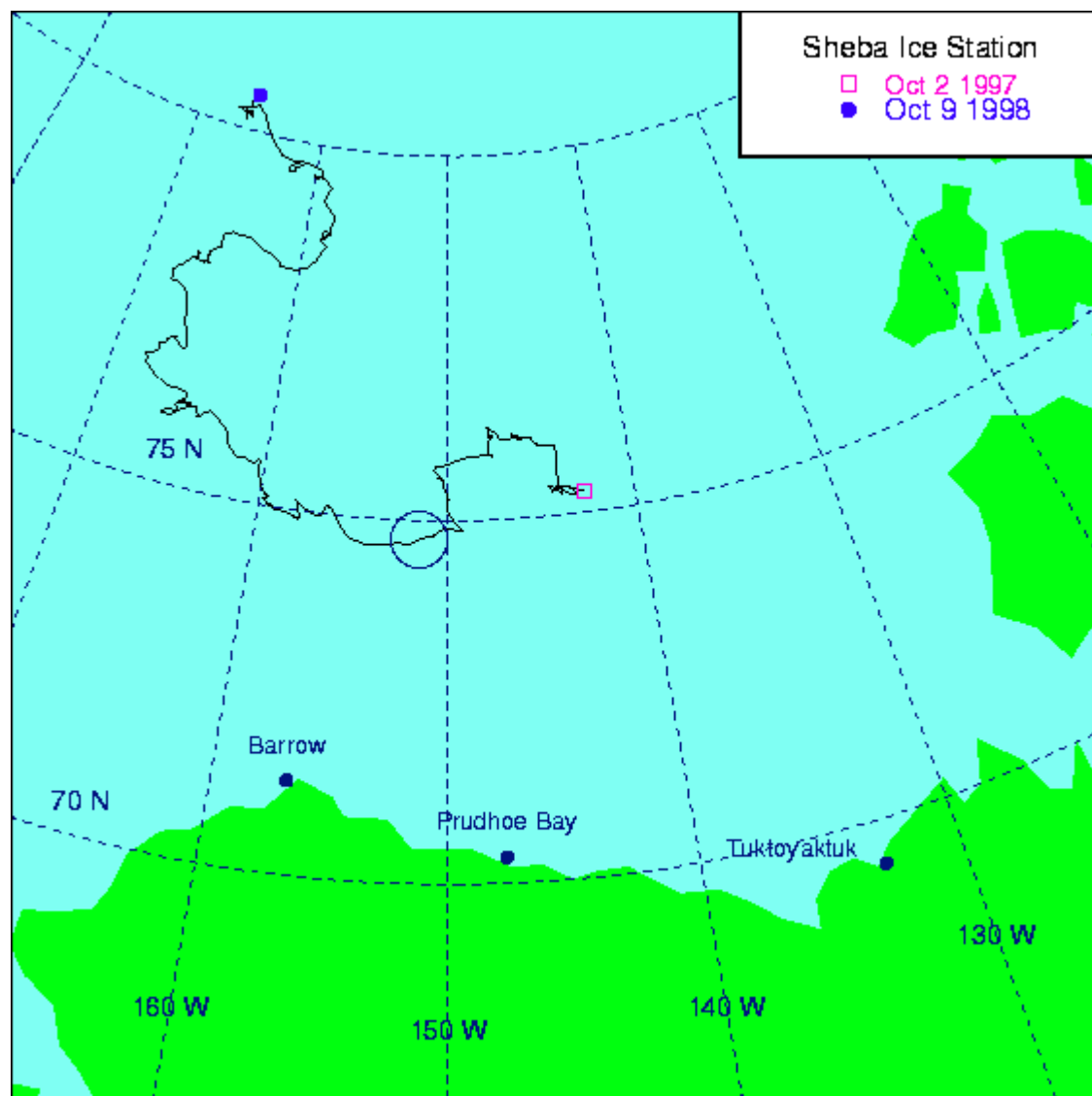
Case	h , m	S , $W\ m^{-2}$	E , $W\ m^{-2}$	net IR , $W\ m^{-2}$	H , $W\ m^{-2}$	h_{param} , m	error in h_{param} , %
Dry	~580	311	n/a	n/a	311	~544	-6.2
Moist	~650	328	107	n/a	435	~608	-6.5
Rad	~710	349	112	105	566	~664	-6.5

^aThe moist case includes the effects of microphysics, and the “rad” case includes radiative effects (all for a 6400 m lead with no large-scale cross-lead wind).

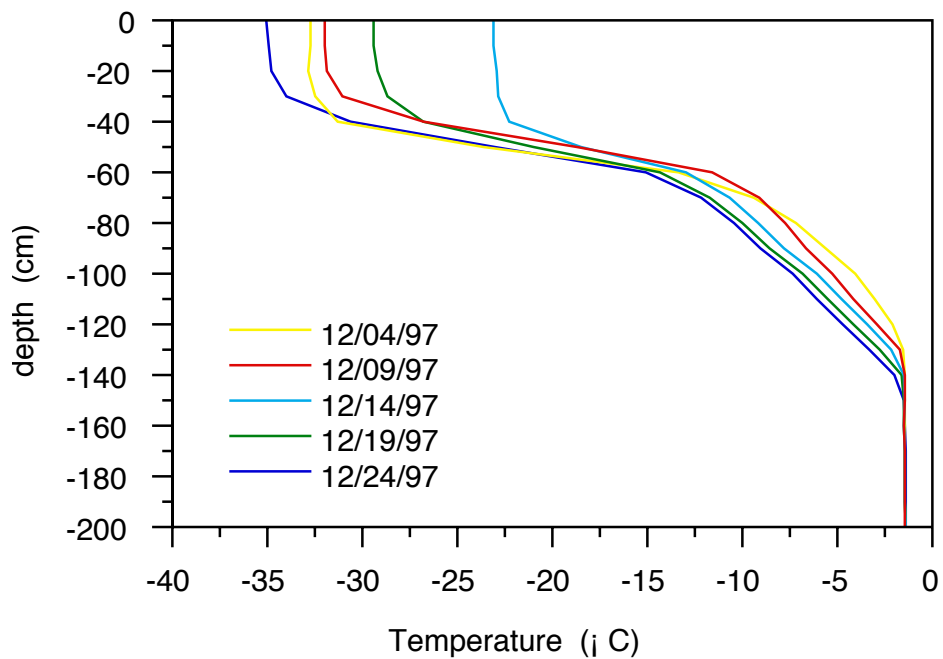
The SHEBA Ice Station



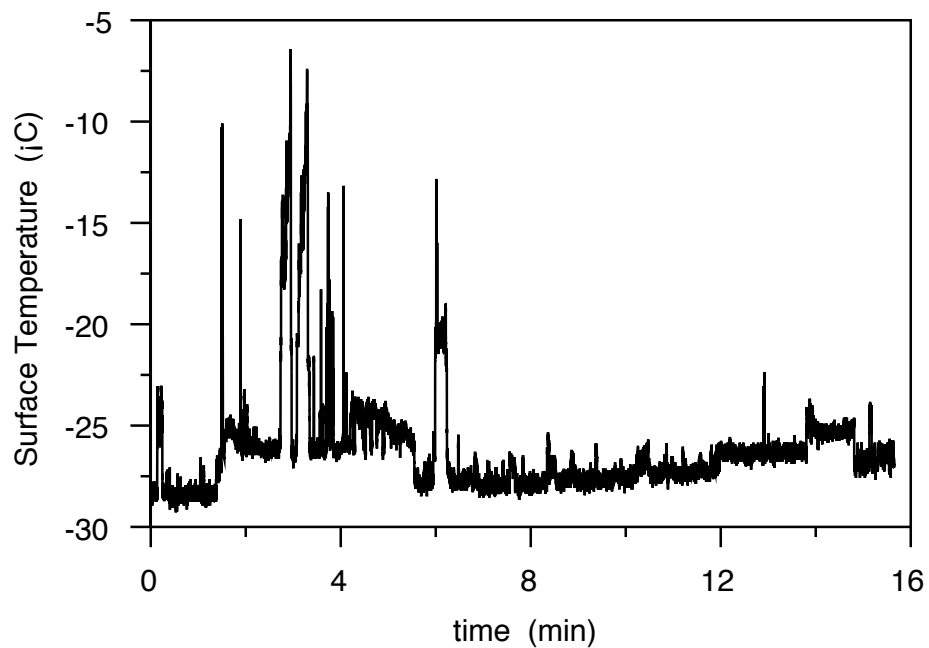
SHEBA Ice Station Drift Track







Snow/ice temperature profiles from Baltimore PAM site, December 1997.



Short segment of surface temperature derived from ferry aircraft radiometer.

Methodology:

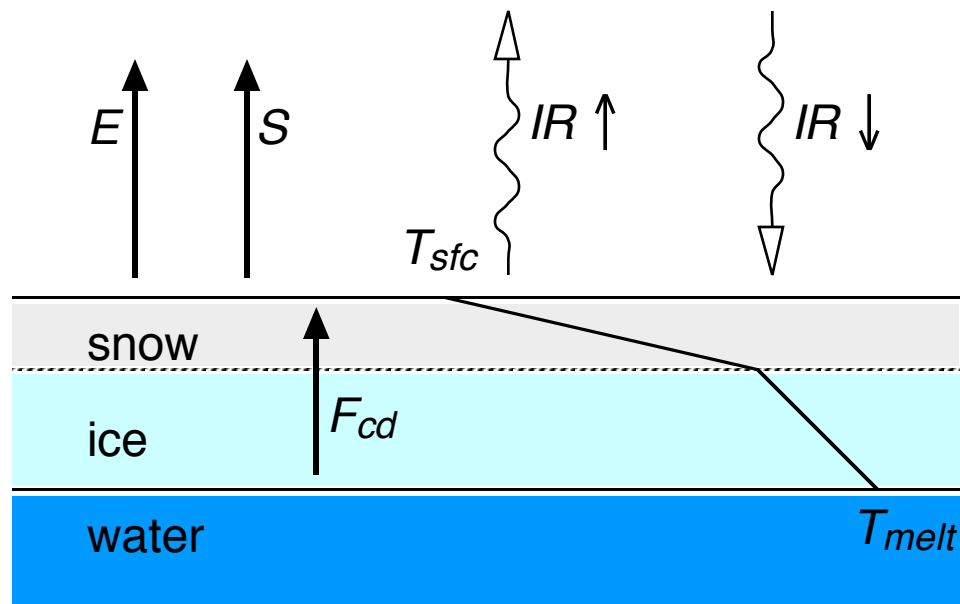
- Modify the UU CRM to more accurately model T_{sfc} and the surface energy balance on snow/ice
- Design a “typical” mid-winter case based on SHEBA observations (Surface Heat Budget of the Arctic Ocean)
- Use the CRM in 2-D mode to resolve and model atmospheric circulations that form in response to a large lead under mid-winter conditions
- Use the CRM in 1-D mode to examine “mosaic” parameterization
- Examine the impact of convective plumes upon large-scale surface fluxes

Most previous studies have handled T_{sfc} very simplistically (ie. T_{sfc} held constant on snow/ice).

To accurately model surface fluxes, an improved surface temperature formulation is required.

T_{sfc} is diagnosed to satisfy energy balance at the surface:

$$F_{cd} = (IR \uparrow - IR \downarrow) + S + E$$

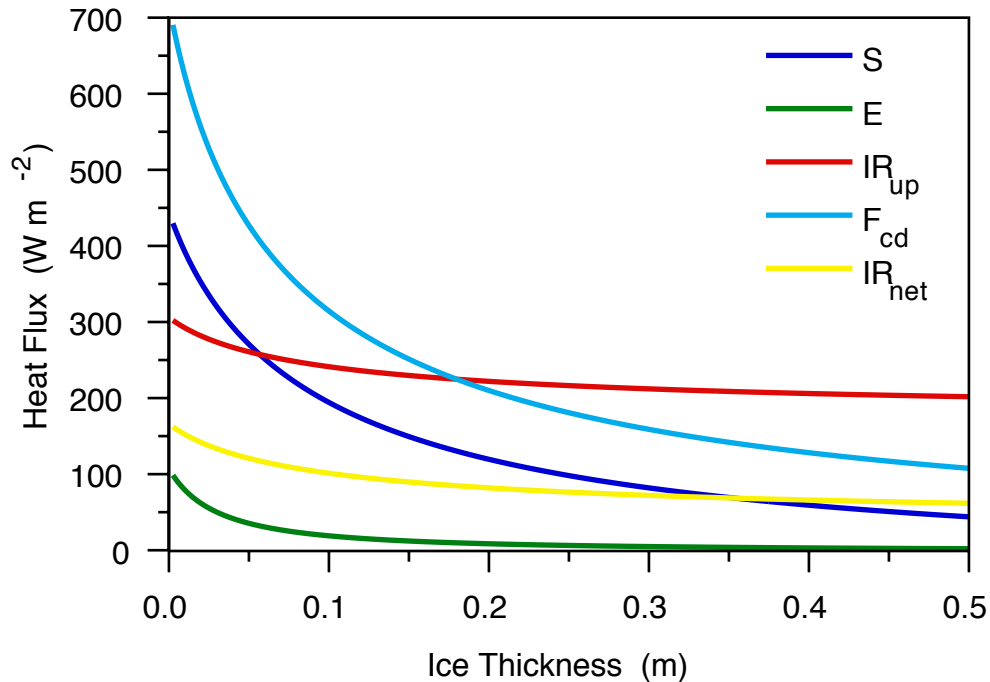


Conductive heat flux is calculated using the internal snow/ice temperature profile, which is integrated in time using the one-dimensional heat equation:

$$(\rho c) \frac{\partial T}{\partial t} = \frac{\partial}{\partial z} \left(k \frac{\partial T}{\partial z} \right)$$

Each surface point is assigned depths of snow and ice, each with respective values for density (ρ), heat capacity (c), and thermal conductivity (k).

Thin ice on partially refrozen leads still allows for significantly enhanced surface fluxes.



The parameters used in calculating this balance are:

- $IR \downarrow = 140 \text{ W m}^{-2}$
- $T_{air} = 240 \text{ K}$
- RH = 80% with respect to liquid water
- 10 m wind $U = 5 \text{ m s}^{-1}$
- $z_0 = 2 \times 10^{-4} \text{ m}$

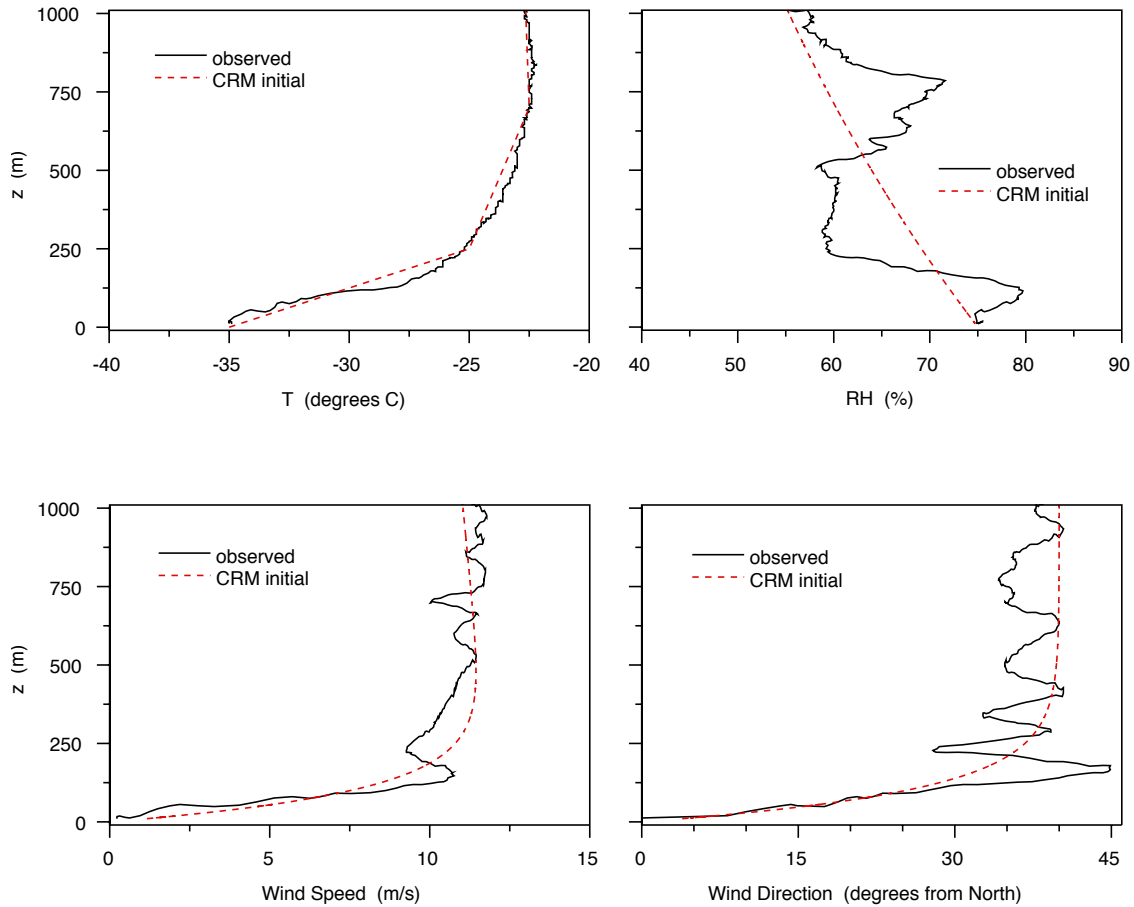
Modeling the evolution of surface temperature: effects on surface fluxes

	T_{sfc} prescribed			T_{sfc} diagnosed		
	water	ice	LS	water	ice	LS
S	260.0	-2.1	30.6	260.0	-14.7	19.6
E	78.6	0.0	9.8	78.6	-0.5	9.4
$IR \uparrow$	305.7	201.3	214.3	305.7	163.7	181.5
$IR \downarrow$	132.0	131.9	131.9	132.0	131.5	131.5
<i>net</i>	512.4	67.3	122.9	512.4	17.1	79.0

“Background” surface fluxes calculated for simulations in which the surface temperature of the ice/snow is prescribed as a constant, and in which it is diagnosed. Large-scale (LS) values calculated using an area-average as in a GCM type parameterization ($f_{lead} = 12.5\%$).

	T_{sfc} prescribed			T_{sfc} diagnosed		
	water	ice	LS	water	ice	LS
S	333.6	-3.7	38.5	353.3	-13.4	32.4
E	103.3	-0.1	12.9	103.5	-0.5	12.5
$IR \uparrow$	305.7	201.3	214.3	305.7	166.6	183.9
$IR \downarrow$	193.8	140.0	146.8	196.4	138.9	146.1
<i>net</i>	548.7	57.5	118.9	566.0	13.8	82.8

Same as above, except for simulations that explicitly resolve a 3.2 km lead and lead-induced circulation in a 25.6 km domain ($f_{lead} = 12.5\%$). Large-scale wind of 2.5 m s^{-1} oriented parallel to lead.

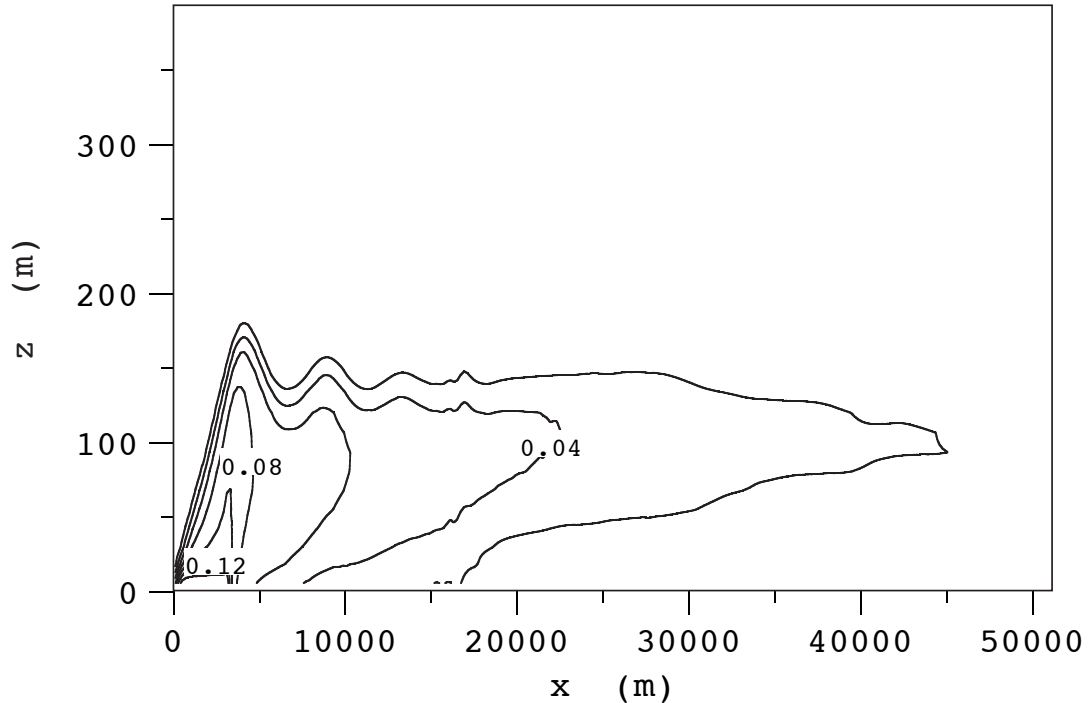


Observed atmospheric soundings from SHEBA rawinsondes for Jan 18, 1998, 23:16 UTC, and the simplified profiles used in initializing the CRM.

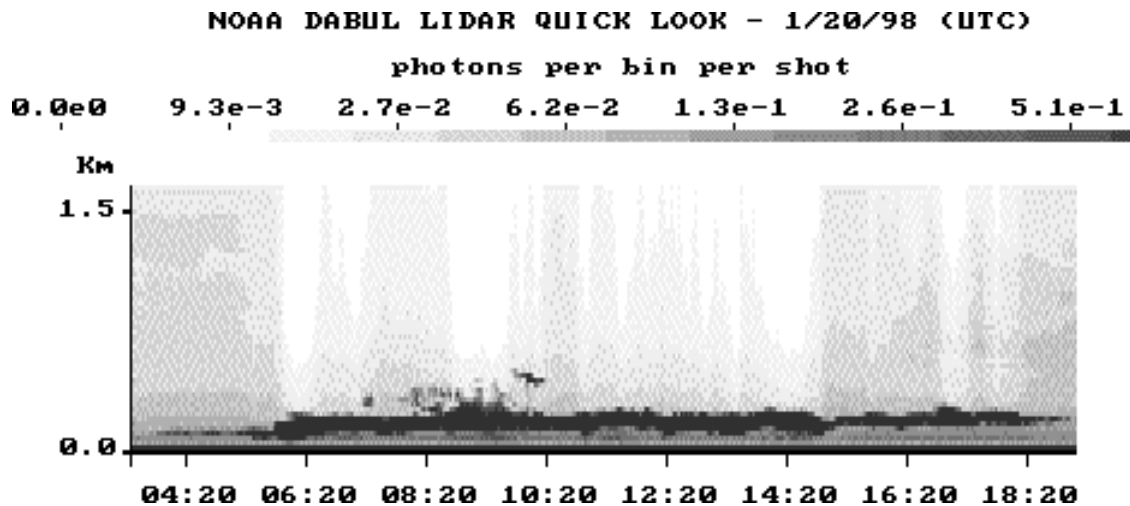
Specifics:

- 256 points in horizontal direction, 200 m resolution (51.2 km domain width)
- 80 points in vertical direction, stretched grid with 12 m resolution near the surface (1.44 km domain height)
- dynamics time step of 1.25 s
- radiative and snow/ice thermal time step of 120 s
- statistics examined after 1.5 hours (wrap-around)

Cloud ice for basic simulation of 3.2 km lead ($f = 6.25\%$) after 1.5 hours.

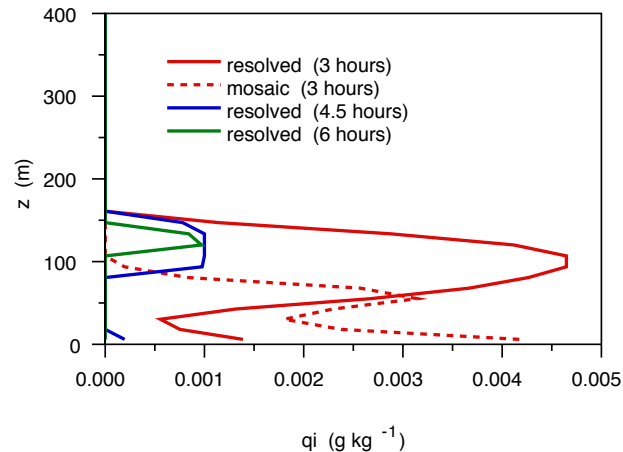


LIDAR imagery from the SHEBA site for January 20, 1998.



Longer term evolution of “mosaic” and resolved lead simulations

Extending the results from the these simulations to longer runs, with lead closure at 1.5 hours:



By 4.5 hours (3 hours after lead closure), cloud ice in “mosaic” simulation has dissipated; cloud ice persists in resolved lead simulation beyond 6 hours.

“Mosaic” Method for Parameterizing Lead Effects in Large-Scale Models

- Calculate fluxes over snow/ice and open water in a grid box using the (same) large-scale atmospheric properties
- Modify the large-scale atmospheric properties using the area-weighted average of the fluxes over snow/ice and open water in a grid box

Table 4: Relevant quantities for forcing fluxes, averaged over leads for various simulations. Columns refer to simulations as described in Table 1.

		initial	resolved	mosaic	1.6 km	6.4 km	thin ice	low RH
U	(m s ⁻¹)	2.9	6.2	4.5	4.9	7.8	5.4	6.1
T_{air}	(K)	238.4	242.2	241.0	240.6	244.2	241.7	242.0
T_{sfc}	(K)	271.1	271.1	271.1	271.1	271.1	261.5	271.1
T_{sky}	(K)	217.3	231.8	226.0	227.5	237.6	225.3	226.2

Table 5: Relevant quantities for forcing fluxes, averaged over snow/ice for various simulations. Columns refer to simulations as described in Table 1.

		initial	resolved	mosaic	1.6 km	6.4 km	thin ice	low RH
U	(m s ⁻¹)	2.9	3.3	4.5	3.1	3.3	3.2	3.3
T_{air}	(K)	238.4	237.6	241.0	236.7	238.7	237.0	237.1
T_{sfc}	(K)	229.9	233.0	235.2	231.2	235.1	231.3	231.1
T_{sky}	(K)	217.3	225.8	225.0	221.5	231.0	220.9	220.4

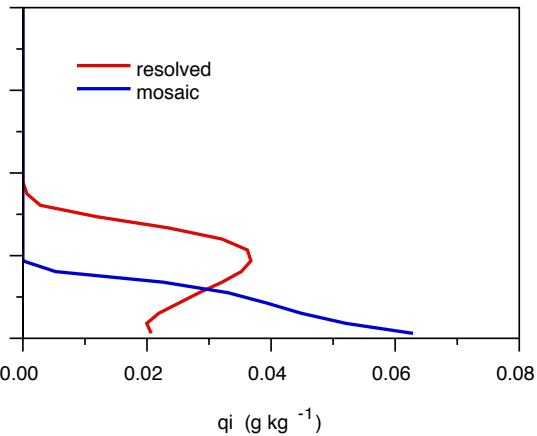
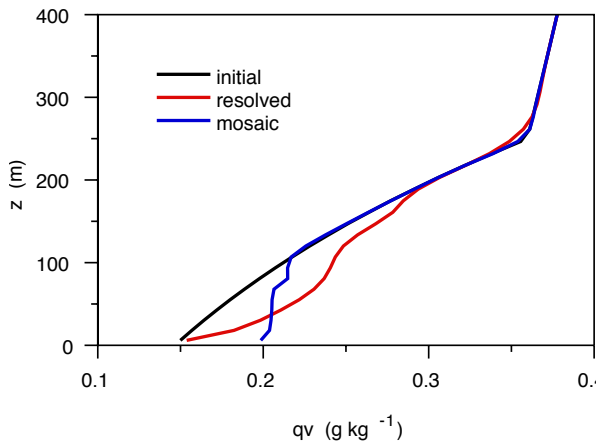
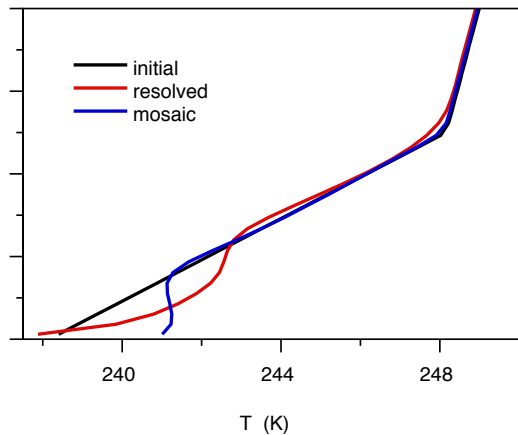
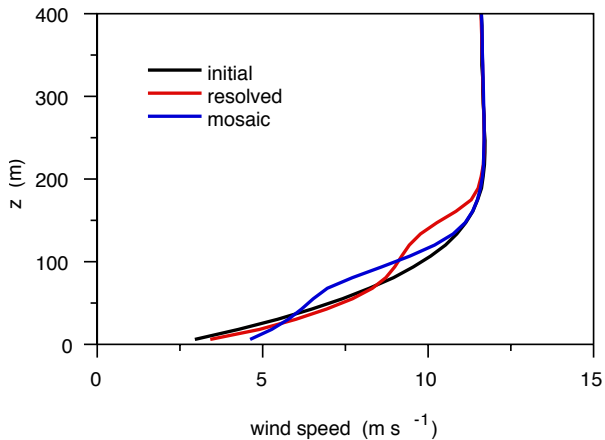


Table 1: Average surface fluxes over leads for various simulations, all values in W m^{-2} . The columns correspond with the following simulations, respectively: the “initial” conditions for the basic simulation, the basic “resolved” lead simulation, the “mosaic” method parameterization, a 1.6-km-wide resolved lead, a 6.4-km-wide resolved lead, a resolved lead covered by a thin 2.5 cm ice layer, and a resolved lead with a lower initial relative humidity. Except for the “initial” column, all results are calculated at 1.5 h.

	initial	resolved	mosaic	1.6 km	6.4 km	thin ice	low RH
S_{ld}	486	691	579	620	754	562	681
E_{ld}	114	168	141	146	191	79	168
$IR \uparrow_{ld}$	306	306	306	306	306	265	306
$IR \downarrow_{ld}$	127	164	149	152	181	146	149
net IR_{ld}	179	141	157	154	125	119	157
net \uparrow flux	779	1000	878	920	1069	759	1005

Table 2: Average surface fluxes over snow/ice for various simulations, all values in W m^{-2} . Columns refer to simulations as described in Table 1.

	initial	resolved	mosaic	1.6 km	6.4 km	thin ice	low RH
S_{ice}	-15	-14	-30	-13	-14	-15	-17
E_{ice}	0	-1	-2	-1	-1	-1	-1
$IR \uparrow_{ice}$	158	167	174	162	174	163	162
$IR \downarrow_{ice}$	127	148	146	137	162	135	134
net IR_{ice}	32	20	27	25	11	27	28
net \uparrow flux	16	5	-4	12	-4	11	11

Table 3: Large-scale surface flux averages for various simulations, all values in W m^{-2} . Columns refer to simulations as described in Table 1.

	initial	resolved	mosaic	1.6 km	6.4 km	thin ice	low RH
S_{ls}	16	30	8	7	82	21	27
E_{ls}	7	10	7	4	23	4	10
$IR \uparrow_{ls}$	168	176	182	167	190	169	171
$IR \downarrow_{ls}$	127	149	146	137	165	136	135
net IR_{ls}	41	27	36	29	26	33	36
net \uparrow flux	64	67	51	40	131	58	73

Conclusions

- The surface temperature must be allowed to evolve to realistically depict the surface energy budget.
- Recently frozen leads have thin ice with substantial sensible heat fluxes, though reduced latent heat fluxes.
- In response to a large lead, the CRM develops a low-level (though still elevated) ice cloud plume, similar to those observed by lidar.
- The mosaic parameterization produces a quite different, surface-based plume.
- Lead-generated plumes and their feedbacks to the surface heat budget result from lead-scale surface, turbulent, microphysical, and radiative processes.

Four basic simulations

1. resolved lead

- 3.2 km resolved lead in 51.2 km domain
- $f = 6.25\%$

2. simple

- fluxes calculated over unbroken water/ice surfaces
- large-scale fluxes calculated using area-weighted average assuming $f = 6.25\%$
- no feedback exists between the over-water fluxes and the over-snow fluxes
- fluxes are calculated using the initial conditions, and do not evolve in time

3. mosaic

- fluxes calculated over unbroken water/ice surfaces
- large-scale fluxes calculated using area-weighted average assuming $f = 6.25\%$
- feedbacks do exist between the over-water fluxes and the over-snow fluxes
- atmospheric conditions, and thus surface fluxes, do evolve in time

4. thin ice

- 3.2 km resolved lead in 51.2 km domain
- $f = 6.25\%$
- lead is covered with 2.5 cm of ice, reducing air-surface temperature difference